Planar photonic crystal cavities with far-field optimization for high coupling efficiency and quality factor

S. L. Portalupi,[1] **M. Galli,**[1] **C. Reardon,**[2] **T. F. Krauss,**[2] **L. O'Faolain,**[2] **L. C. Andreani,**[1] **and D. Gerace**[1,*]

[1] *Dipartimento di Fisica "A. Volta," Università di Pavia, via Bassi 6, 27100 Pavia, ITALY*
[2] *School of Physics and Astronomy, University of St. Andrews, Fife KY169SS, St. Andrews, UK*
[*] *dario.gerace@unipv.it*

Abstract: Different types of planar photonic crystal cavities aimed at optimizing the far-field emission pattern are designed and experimentally assessed by resonant scattering measurements. We systematically investigate the interplay between achieving the highest possible quality (Q) factor and maximizing the in- and out-coupling efficiency into a narrow emission cone. Cavities operate at telecommunications wavelengths, i.e. around $\sim 1.55\ \mu$m, and are realized in silicon membranes. A strong modification of the far-field emission pattern, and therefore a substantial increase of the coupling efficiency in the vertical direction, is obtained by properly modifying the holes around L3, L5 and L7 type PhC cavities, as we predict theoretically and show experimentally. An optimal compromise yielding simultaneously a high Q-factor and a large coupling to the fundamental cavity mode is found for a L7-type cavity with a measured $Q \simeq 62000$, whose resonant scattering efficiency is improved by about two orders of magnitude with respect to the unmodified structure. These results are especially useful for prospective applications in light emitting devices, such as nano-lasers or single-photon sources, in which vertical in- and out-coupling of the electromagnetic field is necessarily required.

OCIS codes: (230.5750) Photonic crystals; (350.4238) Nanophotonics and photonic crystals.

References and links

1. J. D. Joannopoulos, S. G. Johnson, J. N. Winn, and R. D. Meade, *Photonic Crystals: Molding the Flow of Light.* (Princeton University Press, Princeton, 2008).
2. A. Badolato, K. Hennessy, M. Atatüre, J. Dreiser, E. Hu, P. M. Petroff, and A. Imamoğlu, "Deterministic coupling of single quantum dots to single nanocavity modes," Science **308**, 1158–1161 (2005).
3. D. Englund, D. Fattal, E. Waks, G. Solomon, B. Zhang, T. Nakaoka, Y. Arakawa, Y. Yamamoto, and J. Vučković, "Controlling the spontaneous emission rate of single quantum dots in a two-dimensional photonic crystal," Phys. Rev. Lett. **95**, 013904 (2005).
4. S. Noda, M. Fujita, and T. Asano, "Spontaneous-emission control by photonic crystals and nanocavities," Nat. Photon. **1**, 449–458 (2007).
5. S. Strauf, K. Hennessy, M. T. Rakher, Y.-S. Choi, A. Badolato, L. C. Andreani, E. L. Hu, P. M. Petroff, and D. Bouwmeester, "Self-tuned quantum dot gain in photonic crystal lasers," Phys. Rev. Lett. **96**, 127404 (2006).
6. M. Notomi, A. Shinya, S. Mitsugi, E. Kuramochi, and H. Ryu, "Waveguides, resonators and their coupled elements in photonic crystal slabs," Opt. Express **12**, 1551–1561 (2004).
7. M. Notomi, A. Shinya, S. Mitsugi, G. Kira, E. Kuramochi, and T. Tanabe, "Optical bistable switching action of Si high-Q photonic-crystal nanocavities," Opt. Express **13**, 2678–2687 (2005).

#129285 - $15.00 USD Received 1 Jun 2010; revised 25 Jun 2010; accepted 5 Jul 2010; published 14 Jul 2010

8. M. Belotti, J. Galisteo-Lopez, S. De Angelis, M. Galli, I. Maksymov, L. C. Andreani, D. Peyrade, and Y. Chen, “All-optical switching in 2D silicon photonic crystals with low loss waveguides and optical cavities,” Opt. Express **16**, 11624–11636 (2008).
9. K. Srinivasan and O. Painter, “Momentum Space Design of High-Q Photonic Crystal Optical Cavities,” Opt. Express **10**, 670–684 (2002).
10. D. Englund, I. Fushman, and J. Vučković, “General recipe for designing photonic crystal cavities,” Opt. Express **13**, 5961–5975 (2005).
11. L. C. Andreani, D. Gerace, and M. Agio, “Gap maps, diffraction losses, and exciton-polaritons in photonic crystal slabs,” Photon. Nanostruct. Fundam. Appl. **2**, 103–110 (2004).
12. Y. Akahane, T. Asano, B. S. Song, and S. Noda, “High-Q photonic nanocavity in a two-dimensional photonic crystal,” Nature **425**, 944–947 (2003).
13. B. S. Song, S. Noda, T. Asano, and Y. Akahane, “Ultra-high-Q photonic double-heterostructure nanocavity,” Nat. Mater. **4**, 207–210 (2005).
14. E. Kuramochi, M. Notomi, S. Mitsugi, A. Shinya, T. Tanabe, and T. Watanabe, “Ultrahigh-Q photonic crystal nanocavities realized by the local width modulation of a line defect,” Appl. Phys. Lett. **88**, 041112 (2006).
15. C. Sauvan, Ph. Lalanne, and J. P. Hugonin, “Slow-wave effect and mode-profile matching in photonic crystal microcavities,” Phys. Rev. B **71**, 165118 (2005).
16. S. Combrié, A. De Rossi, Q. V. Tran, and H. Benisty, “GaAs photonic crystal cavity with ultra-high Q: microwatt nonlinearity at 1.55 μm,” Opt. Lett. **33**, 1908–1910 (2008).
17. K. Srinivasan, P. E. Barclay, M. Borselli, O. Painter, “Optical-fiber-based measurement of an ultra-small volume high-Q photonic crystal microcavity,” Phys. Rev. B **70**, 081306(R) (2004).
18. P. E. Barclay, K. Srinivasan, and O. Painter, “Nonlinear response of silicon photonic crystal micresonators excited via an integrated waveguide and fiber taper,” Opt. Express , **13** 801–820 (2005).
19. S. G. Johnson, S. Fan, A. Mekis, and J. D. Joannopoulos, “Multipole-cancellation mechanism for high-Q cavities in the absence of a complete photonic band gap,” Appl. Phys. Lett. **78**, 3388–3390 (2001).
20. S.-H. Kim, S.-K. Kim, and Y.-H. Lee “Vertical beaming of wavelength-scale photonic crystal resonators,” Phys. Rev. B **73**, 235117 (2006).
21. F. Römer and B. Witzigmann, “Spectral and spatial properties of the spontaneous emission enhancement in photonic crystal cavities,” J. Opt. Soc. Am. B **25**, 31–39 (2008).
22. M. Larque, T. Karle, I. Robert-Philipp, and A. Beveratos, “Optimizing H1 cavities for the generation of entangled photon pairs,” New J. Phys. **11**, 033022 (2009).
23. N.-V.-Q. Tran, S. Combrié, and A. De Rossi, “Directive emission from high-Q photonic crystal cavities through band folding,” Phys. Rev. B **79**, 041101(R) (2009).
24. M. Toishi, D. Englund, A. Faraon, and J. Vučković, “High-brightness single photon source from a quantum dot in a directional emission nanocavity,” Opt. Express **17**, 14618–14626 (2009).
25. M. McCutcheon, G. W. Rieger, I. W. Cheung, J. F. Young, D. Dalacu, S. Frédéric, P. J. Poole, G. C. Aers, and R. Williams, “Resonant scattering and second-harmonic spectroscopy of planar photonic crystal microcavities,” Appl. Phys. Lett. **87**, 221110 (2009).
26. M. Galli, S. L. Portalupi, M. Belotti, L. C. Andreani, L. O’Faolain, and T. F. Krauss, “Light scattering and Fano resonances in high-Q photonic crystal nanocavities,” Appl. Phys. Lett. **94**, 071101 (2009).
27. P. Deotare, M. McCutcheon, I. Frank, M. Khan, and M. Loncar, “High quality factor photonic crystal nanobeam cavities,” Appl. Phys. Lett. **94**, 121106 (2009).
28. D. Gerace and L. C. Andreani, “Effects of disorder on propagation losses and cavity Q-factors in photonic crystal slabs,” Photon. Nanostruct. Fundam. Appl. **3**, 120–128 (2005).
29. L. C. Andreani and D. Gerace, “Photonic crystal slabs with a triangular lattice of triangular holes investigated using a guided-mode expansion method,” Phys. Rev. B **73**, 235114 (2006).
30. Commercial FDTD software from Lumerical Solutions Inc. has been partly used for the 3D FDTD simulations reported in this work.
31. L. O’Faolain, X. Yuan, D. McIntyre, S. Thoms, H. Chong, R. M. De La Rue and T. F. Krauss, “Low-loss propagation in photonic crystal waveguides,” Electron. Lett. **42**, 1454–1455 (2006).
32. A. Witvrouwa, B. Du Bois, P. De Moor, A. Verbist, C. Van Hoof, H. Bender, K. Baert, “A comparison between wet HF etching and vapor HF etching for sacrificial oxide removal,” Proc. SPIE **4174** 130–141 (2000).
33. D. Gerace, H. E. Türeci, A. Imamoğlu, V. Giovannetti, and R. Fazio, “The quantum optical Josephson interferometer,” Nat. Phys. **5**, 281–284 (2009).

1. Introduction

Planar photonic crystal (PPhC) cavities [1] have become a fundamental tool in modern photonics research, either for investigating basic cavity quantum electrodynamics effects [2–5] or for developing prospective nanophotonic devices for all-optical integration [6–8]. One key feature of such nanocavities is the figure of merit represented by the ratio Q/V_{eff} between the cavity mode quality factor and its effective confinement volume. In fact, ultra-high Q-factors have been proposed [9–11] and experimentally achieved [12–14] with a variety of different PPhC cavity designs, together with unprecedented small (diffraction-limited) V_{eff}.

However, even if such ultra-high-Q cavities are very well suited for in-plane applications on photonic chips, a major issue might be represented by their off-plane radiation pattern, which makes vertical in- and out-coupling difficult. Q-factor optimization mostly relies on the widespread strategy of reducing the Fourier components of the cavity mode profile within the light cone to achieve a "gentle confinement" [12] by means of a local geometry adjustment. Quite intuitively, this corresponds to reducing the coupling to radiative modes, which is the major source of losses in such systems. The Q-factor optimization can also be interpreted in terms of Bloch mode profile matching [15]. Typical cavity designs that have been proposed and have become widely used among the groups involved in nanophotonic research in last few years are: Ln cavities [12], with n missing holes along the ΓK direction in a triangular lattice, heterostructure cavities [13] and modulated width cavities [14], in which a localized shifting of holes along a photonic crystal waveguide produces a strong field confinement in the propagation direction. This approach is particularly well suited for fully integrated devices in which efficient coupling of electromagnetic energy into the cavity region can be achieved through evanescent excitation from an access waveguide [13, 14, 16] or a fiber taper [17, 18]. However, many applications and research directions employing PPhC cavities require an optimized out-coupling (e.g., in emission experiments, such as photoluminescence from active media within the PPhC) or in-coupling efficiency (e.g., in optically pumped nanophotonic devices) along the direction orthogonal to the slab plane, or both (e.g., when excitation and emission are collected through the same optical channel). Nevertheless, very few researchers have considered possible strategies towards an optimization of far-field coupling for PPhC cavity modes after some early attempts to achieve a high-Q cavity design by reducing the out-coupling efficiency and simultaneously manipulating the far-field profile [19]. Among them, Kim et al. [20] have discussed far-field optimization of hexapole modes in H1 cavities (i.e. a single missing hole in a triangular lattice), by properly placing a distributed-Bragg reflector below the membrane to get constructive interference of the vertically emitted beam. To the best of our knowledge, Ref. [21] is the first systematic numerical study of simultaneous Q-factor and far-field optimization, mainly for the H1-type cavity (see, e.g., Fig. 3 in the latter work). Optimization of H1-type cavity far-field has been also addressed more recently in Ref. [22]. However, H1-type cavities intrinsically suffer from a relatively limited maximum achievable Q-factor. Working on cavity modes with a larger theoretical Q, Tran et al. have proposed a grating approach to concentrate light emission from a L5 cavity around the vertical direction [23], thus enhancing the out-coupling efficiency (with excitation in the plane through an access waveguide). The same concepts have been used for a L3-type cavity in Ref. [24] to demonstrate an efficient single photon source with a single quantum dot. In the latter, a useful collection efficiency in the far-field could be achieved together with Q-factors on the order of 10^4.

Here, we experimentally verify a systematic approach to simultaneously achieving the highest possible Q-factor and an enhanced in- and out-coupling efficiency. We employ PPhC cavities of the Ln type fabricated on a standard Silicon-on-Insulator (SOI) chip, targeting operation at the telecommunications wavelengths (i.e. around 1.55 μm). We elaborate on the simple idea described in Refs. [23, 24], but explore the entire parameter space of PPhC cavity design in order to find the best possible compromise. Our modelling is confirmed by an experimental characterization of both Q-factor and coupling efficiency through resonant scattering measurements [25–27].

The paper is organized as follows: in Sec. 2 we recall the design strategy for Q-factor and far-field optimization, in Sec. 3 we describe sample fabrication and show our experimental results

#129285 - $15.00 USD Received 1 Jun 2010; revised 25 Jun 2010; accepted 5 Jul 2010; published 14 Jul 2010

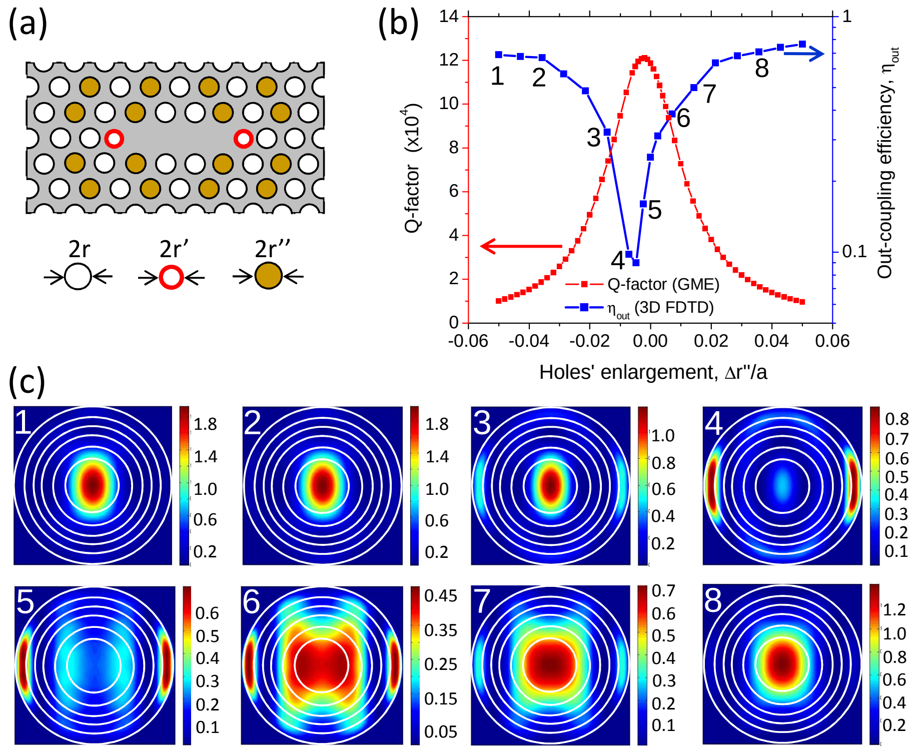

Fig. 1. (a) Schematic of far-field optimized PPhC cavity of the L3-type. Holes with red edge are shrunk and shifted to optimize the Q-factor. Dark holes are modified to increase the vertical out-coupling. (b) Calculated Q-factor and out-coupling efficiency (η_{out}) as a function of the filled holes' radius enlargement. Parameters of the basic PPhC structure are: membrane thickness $d = 220$ nm, lattice constant $a = 420$ nm, photonic crystal holes' radius $r/a = 0.265$, refractive index of dielectric slab $n_{\mathrm{diel}} = 3.46$, red holes shift $\Delta x/a = 0.16$, shrink $\Delta r'/a = -0.06$. (c) A selection of calculated far-field patterns (electric field intensity profile, $|\mathbf{E}|^2$) corresponding to the labeled numbers on the efficiency plot (see numbers in panel b). Field intensities are normalized to the total emitted power in the vertical half-space. Concentric circles correspond to $\theta = 20^\circ, 30^\circ, 40^\circ, 50^\circ, 60^\circ, 90^\circ$ from the inner to the outer one, respectively.

on the optical characterization of the fabricated devices, together with a discussion on its main outcome in Sec. 4. Finally, we analyze the implications of this work in Sec. 5.

2. Theoretical modelling: design and simulation

The principle of far-field optimization through the grating effect [23] relies on the consideration that Fourier components lying outside the light cone can be folded back to $k = 0$, i.e. around the normal direction to the sample surface, by superimposing a lattice with twice the periodicity of the underlying photonic crystal structure. This way, leakage will be mainly determined by the harmonic components oscillating with a wave-vector $k \sim \pi/a$ of the original lattice, which in the Brillouin zone of the modified lattice with period $2a$ are folded exactly at $k = 0$. For a L3-type cavity, the principle is illustrated in Fig. 1a. We start from a Q-optimized L3 cavity, with nearby holes along ΓK that have been shifted and shrunk by $\Delta x/a = 0.16$ and $\Delta r'/a =$

Received 1 Jun 2010; revised 25 Jun 2010; accepted 5 Jul 2010; published 14 Jul 2010

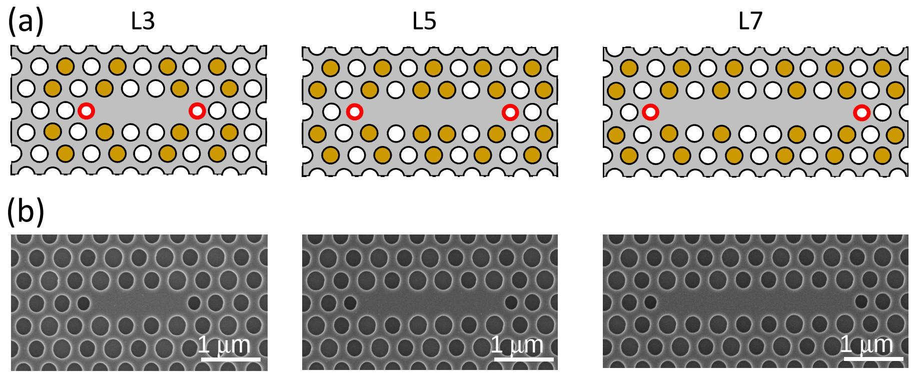

Fig. 2. (a) Schematic pictures of the fabricated PPhC devices: 3, 5, and 7 missing holes define the L3, L5 and L7-type cavities, respectively. Red holes are shifted ($\Delta x/a = 0.16$) and shrunk ($\Delta r'/a = -0.06$) for Q-factor optimization, while dark holes are modified for far-field optimization. (b) SEM images of 3 fabricated devices on silicon membranes. Holes corresponding to the filled circles in (a) are enlarged by $\Delta r'' = 21$ nm in these images. Lattice constant is $a = 420$ nm for all the investigated PPhC devices.

$r' - r = -0.06$, respectively (see also Ref. [11]). In Fig. 1a we show which holes around the cavity region can be modified in order to superimpose a second lattice with periodicity $2a$. As anticipated in Ref. [23], this procedure of far-field optimization is very robust with respect to disorder [28]. In fact, the Fourier components of the L3 cavity mode are always partly folded to $k = 0$, no matter which kind of perturbation one performs on the selected holes. The far-field emission from the PPhC obviously reflects the Fourier spectrum of its real-space electric field intensity profile.

We concentrate, in this Section and in the following ones, on modes of even parity with respect to mirror symmetry through the horizontal plane bi-secting the PPhC membrane (TE-like modes) [11]. A systematic analysis of both the Q-factor and the far-field out-coupling efficiency of the fundamental cavity mode is required in order to find the structural parameters that realize the best compromise. To this end, we show in Fig. 1b the calculated Q-factor as a function of the filled holes' radius modification, $\Delta r'' = r'' - r$: positive hole enlargement ($\Delta r'' > 0$) gives larger holes, while negative one ($\Delta r'' < 0$) is for smaller holes. The Q-factor calculations have been performed with a guided-mode expansion (GME) method [29], which allows a fast scanning of the structure parameters. For a selection of modified holes radii, we show in the same plot the calculated out-coupling efficiency in the far-field. For the latter simulation, we employed a commercial three-dimensional finite-difference time-domain (3D FDTD) software [30]. We simulate the excitation of the cavity mode with an internal dipole source, recorded the near-field intensity at the sample surface, and applied a standard near-to-far-field projection [24,30]. A few normalized far-field patterns are shown in Fig. 1c, clearly displaying the evolution as a function of $\Delta r''/a$. Finally, for the collection efficiency calculation we assumed a filter in the far-field, corresponding to numerical aperture NA=0.5 (which is usually employed in experiments), i.e. a collection angle $\theta \simeq \pm 30^\circ$ around the direction normal to the PPhC surface. In practice, we simulate the collection efficiency of the objective by integrating over a definite solid angle around the normal incidence, corresponding to the given NA, which leads to the quantity defined η_{out}. We assume the filter to be orthogonally polarized with respect to the cavity axis, i.e. parallel to the dominant field component of the PPhC cavity mode.

The results show that modified PPhC of the L3-type should improve out-coupling efficiency

#129285 - $15.00 USD Received 1 Jun 2010; revised 25 Jun 2010; accepted 5 Jul 2010; published 14 Jul 2010

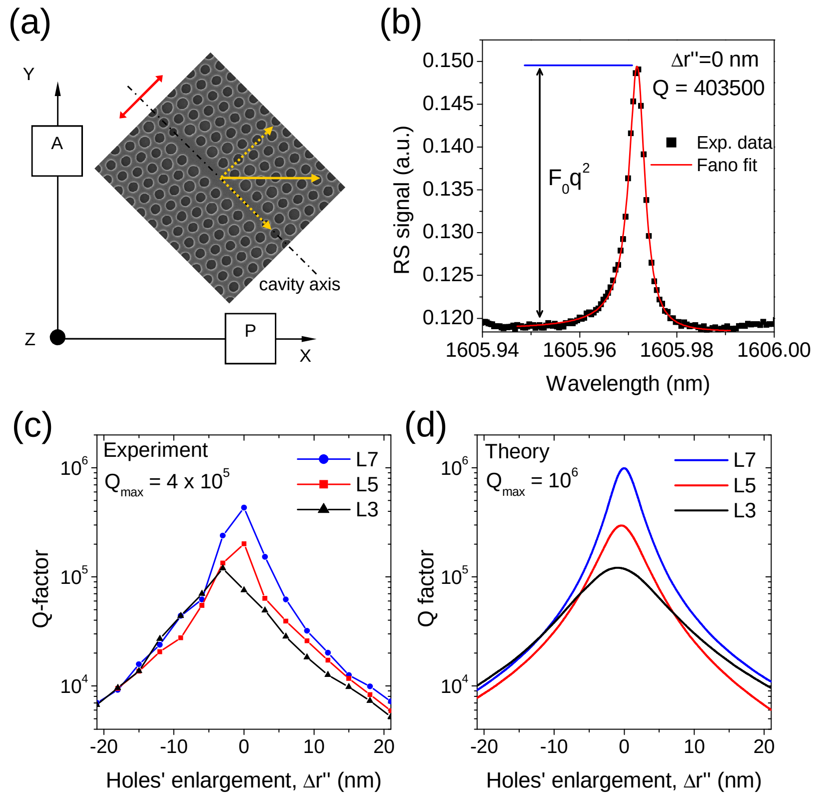

Fig. 3. (a) Schematic illustration of the resonant scattering technique. (b) Resonant scattering signal from a L7 cavity with $\Delta r'' = 0$, showing the largest Q-factor. (c) Measured Q-factor as a function of holes' enlargement for L3, L5, and L7 PPhC devices. (d) Calculated Q-factor (by GME) as a function of holes' enlargement for L3, L5, and L7 PPhC devices.

by a factor of ~ 3.5 as compared to a bare optimized L3 (corresponding to $\Delta r''/a = 0$), and about a factor of ~ 7 as compared to the cavity with $\Delta r''/a \sim -0.01$ that is the one with the minimum out-coupling efficiency. Interestingly and somewhat counter-intuitively, for the L3-type cavity the behavior of both Q-factor and out-coupling efficiency is slightly asymmetric with respect to $\Delta r''$, showing a minimum collection (maximum Q-factor) for $\Delta r'' < 0$. The latter effect is also evident from the far-field intensities of Fig. 1c. As a final comment to these results, we notice that the calculated out-coupling efficiency gain is generally at the expense of a Q-factor reduction. A discussion on the figure of merit leading to the best trade-off between these two quantities will be presented in Sec. 4.

3. Sample fabrication and optical measurements

PPhC are fabricated on a standard SOITEC silicon-on-insulator wafer, with a nominal 220 nm device layer with 2 μm buried oxide, using electron-beam lithography (hybrid ZEISS GEMINI 1530/RAITH ELPHY system) and reactive ion etching with a CHF_3/SF_6 gas mixture (see [31] for details). The buried oxide layer underneath the photonic-crystal slab was selectively underetched using a vapor Hydrofluoric acid method [32] to leave the photonic crystal section as a suspended silicon membrane. The schematic structure designs and the holes to be modified for

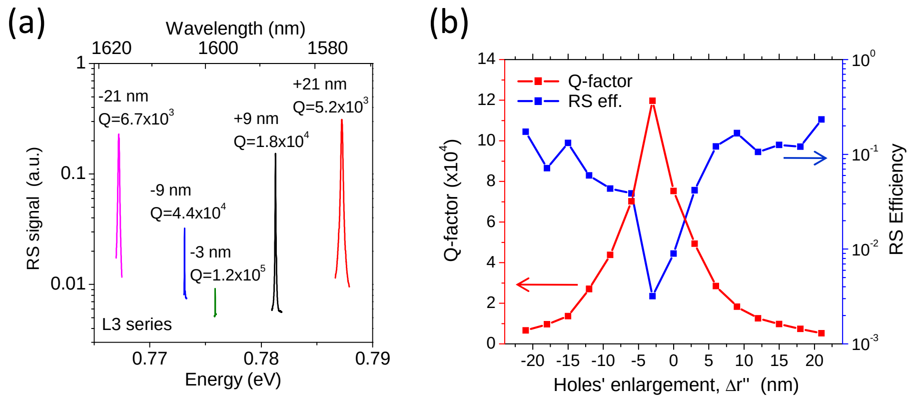

Fig. 4. (a) Sample spectra from resonant scattering measurements on the fundamental mode of L3-type PPhC. (b) The extracted Q-factors and RS efficiencies extracted from the measured data in (a) and plotted as a function of $\Delta r''$, to be compared to Fig. 1(b).

far-field optimization are represented in Fig. 2a. The lattice constant for all devices was 420 nm, with nominal hole radius $r/a \sim 0.28$, and the dimensionless parameters, $\Delta x/a$ and $\Delta r'/a$, were also held constant. The modified holes' radii have been reduced/increased in steps of 3 nm, i.e. from $\Delta r'' = -21$ nm to $\Delta r'' = +21$ nm. The exposure conditions were carefully chosen to allow such precise increments in hole radii. As L3 type PPhCs have maximum Q-factors on the on order of 10^5, we have also designed and fabricated L5 and L7 type PPhC cavities (i.e., 5 and 7 missing holes along ΓK), which nominally have even larger Q-factors. For such cavity types, similar far-field optimization principles hold, promising useful coupling efficiencies at possibly higher Q factors. Figure 2b shows some examples of the fabricated modified PPhCs. Modified holes are also visible in the SEM images.

Optical characterization of the PPhC devices is performed by resonant scattering (RS) from the sample surface. The technique is illustrated in Fig. 3a and detailed in Ref. [26]. Briefly, it consists of measuring reflectance at normal incidence from the PPhC in a crossed-polarization geometry defined by a polarizer (P) and an analyzer (A). The cavity must be oriented at 45° with respect to both P and A in order to achieve simultaneous coupling of incoming and outgoing polarizations with the fundamental cavity mode, therefore maximizing the resonant signal over the background. Asymmetric Fano lineshapes are in general observed and can be fitted with the function

$$F(\omega) = A_0 + F_0 \frac{[q + 2(\omega - \omega_0)/\Gamma]^2}{1 + [2(\omega - \omega_0)/\Gamma]^2}, \tag{1}$$

where q is the Fano parameter which determines the asymmetry of the lineshape and A_0 and F_0 are constant factors. The quality factor is determined as $Q = \omega_0/\Gamma$. Notice that for $q \gg (\omega - \omega_0)/\Gamma$ the Fano lineshape reduces to a symmetric Lorentzian. In this case, the quantity $F_0 q^2$ represents the intensity of the RS signal at resonance with the cavity mode. A typical RS spectrum is shown in Fig. 3b together with the Fano lineshape fit. The Q-factors directly extracted from the RS measurements are reported in Fig. 3c, and compared to the GME calculations in Fig. 3d. A very good agreement can be noticed for all the measured devices. For L3-type PPhC, the maximum Q-factor occurs for $\Delta r'' < 0$, as already anticipated in Fig. 1 and here confirmed experimentally. The maximum theoretical Q-factor ($Q \sim 10^6$) is for the L7-type cavity with $\Delta r'' = 0$. This is confirmed experimentally with the measured $Q \sim 4 \times 10^5$, only a factor of ~ 2 reduced with respect to the one predicted for the ideal L7 PPhC cavity.

#129285 - $15.00 USD Received 1 Jun 2010; revised 25 Jun 2010; accepted 5 Jul 2010; published 14 Jul 2010

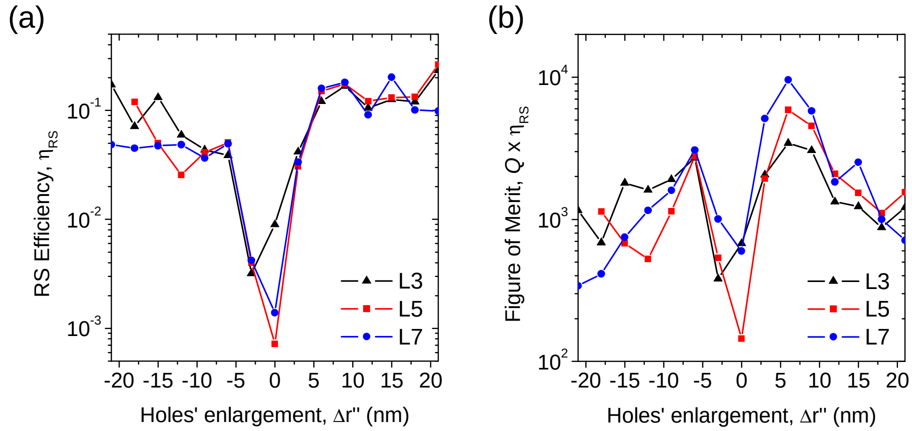

Fig. 5. (a) Experimentally determined RS efficiencies (η_{RS}), for L3, L5, and L7 cavities, respectively, as a function of $\Delta r''$, as measured with a focussing objective having NA=0.5; (b) corresponding figures of merit, given by the product $Q \times \eta_{\mathrm{RS}}$.

The RS measurements have been used also to give a qualitative estimation of the coupling efficiency of our devices. In fact, the quantity $F_0 q^2$ in Eq. (1) is proportional to the light intensity that has been coupled to the cavity mode and reflected back to the detector in crossed polarizations [24]. To normalize this quantity, we determine the intensity I of the incident light by replacing the sample with a nearly ideal dielectric mirror and measuring the reflected intensity, under the same focusing conditions but with parallel polarizations. Thus, we define the RS efficiency as $F_0 q^2/I$. The latter quantity is taken as a measure of cross-polarized scattering due to resonant coupling with the cavity mode (see Fig. 3b).

A few representative RS spectra are shown in Fig. 4a for the L3-type PPhC with different hole modifications. The RS efficiencies, $\eta_{\mathrm{RS}} = F_0 q^2/I$, are reported in Fig. 4b for L3 cavities, together with the corresponding Q-factors. The latter figure should be compared to the theoretically predicted behavior shown in Fig. 1b, which is qualitatively well reproduced from the experimental curves. In particular, the minimum RS efficiency occurs in correspondence with the maximum Q-factor, as anticipated in Fig. 1b. For the L3-type cavity, this happens theoretically for $\Delta r''/a \sim -0.003$; in the experiment, it is the cavity with $\Delta r'' = -3$ nm that simultaneously displays the largest Q-factor and the smallest RS efficiency.

In order to complete our analysis, we show in Fig. 5a the measured RS efficiencies for the whole series of L3, L5, and L7 devices. For all the devices, we refer to their fundamental TE-like cavity mode. In general, the behavior of the RS efficiency as a function of the hole modification is analogous for all the three series of modified cavities, showing a pronounced minimum close to the unmodified cavity and a rapid increase for both positive and negative values of $\Delta r''$. A quantitative comparison between the different devices to infer the best trade-off can be directly made by looking at the relevant figure of merit, i.e. the product of Q-factor (data reported in Fig. 3c) and RS efficiency, which is shown in Fig. 5b. From this plot, we can directly infer that an optimal compromise between Q-factor and RS efficiency is reached for the L7-type cavity with $\Delta r'' = 6$ nm. For this device, we measured $Q \sim 62000$ and a RS efficiency $\eta_{\mathrm{RS}} \sim 16\%$, improved by about two orders of magnitude with respect to the unmodified L7 cavity (i.e., the one with $\Delta r'' = 0$). The figure of merit plotted in Fig. 5b contains the main message of the present work.

#129285 - $15.00 USD Received 1 Jun 2010; revised 25 Jun 2010; accepted 5 Jul 2010; published 14 Jul 2010

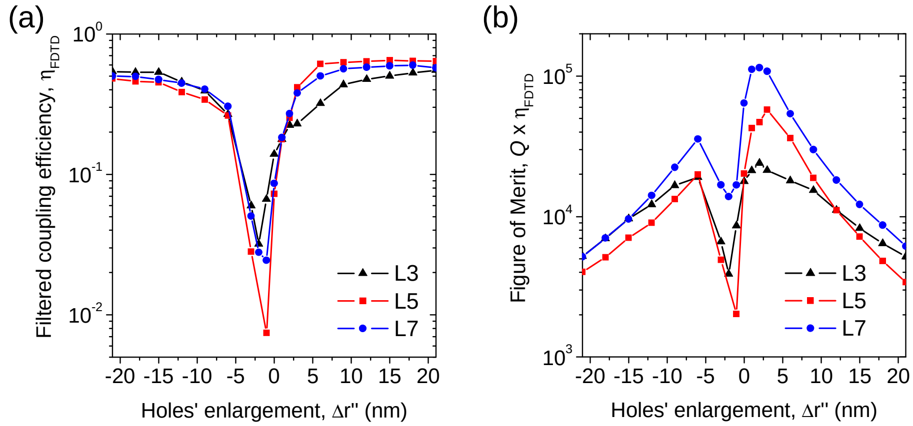

Fig. 6. (a) Modelling of the collection efficiency for L3, L5, and L7 devices (as obtained from 3D FDTD simulations) for an objective with NA=0.5, which has been filtered with a normalized gaussian spot propagated in the far-field whose divergence angle corresponds to the nominal NA (the result is defined η_{FDTD}); (b) the corresponding figures of merit ($Q \times \eta_{\mathrm{FDTD}}$) obtained from the calculated Q-factors (Fig. 3d) for the experimentally realized values of $\Delta r''$.

4. Coupling efficiencies

A direct quantitative comparison between the measured RS efficiency and a theoretically modeled coupling coefficient is a nontrivial task, requiring specific simulation of the RS configuration with in- and out-going focused Gaussian beams that imply a significant increase of convergence issues and computational effort. Moreover, even in presence of such an accurate modelling, extraction of the absolute coupling efficiency to the cavity mode from the RS measurements would not be straightforward. This is due to the combined effect of the specific experimental geometry and the polarization properties of the cavity mode itself, which depend nontrivially on the holes' modification that introduce scattering of field components both parallel and perpendicular to the cavity axis (as we have experimentally verified). This more advanced analysis is beyond the scope of the present manuscript, and it is left for future work.

However, the key figure of merit quantifying the best trade-off between Q-factor and coupling coefficient to the cavity mode can be identified without the need for such an analysis. This is demonstrated in Fig. 5b, where the measured RS efficiency can be taken as an indicative measure of the real coupling efficiency from the external world to the cavity mode, along the lines already reported in previous work [24]. Thus, we can give a qualitative interpretation of the experimental data shown in Fig. 5 by using our FDTD results obtained by exciting the cavity mode through an internal dipole source. To this end, and to approximate the experimental situation as closely as possible, we have assumed a convolution of the normalized cavity mode far-field profile with a (normalized) Gaussian obtained from the near-to-far field propagation of a spot corresponding to the NA used experimentally. The out-coupling efficiency is finally calculated by filtering this convolution at an angle corresponding to the same numerical aperture (standard NA=0.5, i.e. $\theta \sim \pm 30^{\circ}$ around the normal incidence), thus mimicking the finite spatial extension of the collection lens. This quantity is defined as the "filtered" out-coupling efficiency, η_{FDTD}. Results are shown in Fig. 6a for the simulated cavities, corresponding closely to the fabricated devices. Although a comparison of the absolute values reported in Figs. 5a and

#129285 - $15.00 USD Received 1 Jun 2010; revised 25 Jun 2010; accepted 5 Jul 2010; published 14 Jul 2010

6a is not truly justified, we immediately notice that the qualitative behaviors compare fairly well across the entire parameter range. In particular, pronounced minima occur close to the unmodified L5 and L7 cavities, the first cavity type showing an even lower coupling efficiency. The latter effect is very well evidenced both in experiment and theoretical modelling. The figure of merit giving information on the best trade-off between Q-factor and out-coupling efficiency, $Q \times \eta_{\mathrm{FDTD}}$, is reported in Fig. 6b. Also in this case, an overall qualitative agreement between theoretical modelling and experimental data can be recognized. In particular, the L7 cavity shows the best trade-off for values of $\Delta r''$ slightly larger than zero. For the L7 cavity parameters that yield an optimal compromise between Q-factor and RS efficiency (i.e. $\Delta r'' = 6$ nm), theoretical modelling predicts $Q \simeq 10^5$ (see Fig. 3d) and filtered out-coupling efficiency $\eta_{\mathrm{FDTD}} \sim 50\%$. In summary, both experiment and theoretical modelling present the same qualitative behavior of the figure of merit for all the analyzed cavities, yielding concurring values for the cavity geometry giving the best trade-off between Q-factor and coupling efficiency.

5. Conclusions

We have designed, fabricated and characterized a series of silicon PPhC cavities with modified geometry to improve coupling of cavity modes in the far field with an incoming/outgoing beam at telecom wavelengths. A systematic investigation of L3, L5, and L7 cavity geometries by means of guided-mode expansion and 3D FDTD simulations allows us to quantify the Q-factors and the out-coupling efficiency. Measurements of cavity modes by means of resonant light scattering with crossed polarizations yield the cavity Q-factors, which agree very well with the theoretical calculations. Such measurements yield also the RS efficiency, which is strongly enhanced for far-field optimized cavities with suitably modified surrounding holes. Our results demonstrate that far-field optimized PPhC cavities can have simultaneously high coupling efficiency and quality factors. A new, relevant figure of merit has been considered to this end, namely the product of the experimentally determined Q-factor and RS efficiency. In particular, an optimal compromise was found for an L7 cavity with modified holes' radii increased by 6 nm, in which $Q \sim 60000$ and RS efficiency improved by more than 2 orders of magnitude with respect to the unmodified cavity were experimentally measured. The present results can be important for the realization of efficient nano-lasers and single-photon sources, as well as implementation of recent proposals with multi-cavity devices [33], in which high Q-factors and good in- and out-coupling efficiency are simultaneously required in a PPhC-based architecture.

Acknowledgments

D. G. is grateful to A. Imamoğlu for many motivating discussions. Useful discussions with D. Bajoni are gratefully acknowledged. This project was supported by Fondazione Cariplo through project 2007-5259, and by EraNET Nano-Sci project LECSIN. The fabrication was carried out through NanoPix (www.nanophotonics.eu).

#129285 - $15.00 USD Received 1 Jun 2010; revised 25 Jun 2010; accepted 5 Jul 2010; published 14 Jul 2010